Neurobiology of Disease

Structural Abnormalities in the Brains of Human Subjects Who Use Methamphetamine

Paul M. Thompson,[1] **Kiralee M. Hayashi,**[1] **Sara L. Simon,**[2] **Jennifer A. Geaga,**[1] **Michael S. Hong,**[1] **Yihong Sui,**[1] **Jessica Y. Lee,**[1] **Arthur W. Toga,**[1] **Walter Ling,**[2] **and Edythe D. London**[2,3,4]

[1]Laboratory of Neuroimaging, Brain Mapping Division, Department of Neurology, Departments of [2]Psychiatry and Biobehavioral Sciences and [3]Molecular and Medical Pharmacology, and [4]Brain Research Institute, University of California Los Angeles School of Medicine, Los Angeles, California 90095

We visualize, for the first time, the profile of structural deficits in the human brain associated with chronic methamphetamine (MA) abuse. Studies of human subjects who have used MA chronically have revealed deficits in dopaminergic and serotonergic systems and cerebral metabolic abnormalities. Using magnetic resonance imaging (MRI) and new computational brain-mapping techniques, we determined the pattern of structural brain alterations associated with chronic MA abuse in human subjects and related these deficits to cognitive impairment. We used high-resolution MRI and surface-based computational image analyses to map regional abnormalities in the cortex, hippocampus, white matter, and ventricles in 22 human subjects who used MA and 21 age-matched, healthy controls. Cortical maps revealed severe gray-matter deficits in the cingulate, limbic, and paralimbic cortices of MA abusers (averaging 11.3% below control; $p < 0.05$). On average, MA abusers had 7.8% smaller hippocampal volumes than control subjects ($p < 0.01$; left, $p = 0.01$; right, $p < 0.05$) and significant white-matter hypertrophy (7.0%; $p < 0.01$). Hippocampal deficits were mapped and correlated with memory performance on a word-recall test ($p < 0.05$). MRI-based maps suggest that chronic methamphetamine abuse causes a selective pattern of cerebral deterioration that contributes to impaired memory performance. MA may selectively damage the medial temporal lobe and, consistent with metabolic studies, the cingulate–limbic cortex, inducing neuroadaptation, neuropil reduction, or cell death. Prominent white-matter hypertrophy may result from altered myelination and adaptive glial changes, including gliosis secondary to neuronal damage. These brain substrates may help account for the symptoms of MA abuse, providing therapeutic targets for drug-induced brain injury.

Key words: methamphetamine; brain imaging; drug abuse; MRI; cortex; hippocampus; limbic system; memory

Introduction

Methamphetamine (MA) abuse is a growing epidemic worldwide. Over 35 million people regularly use amphetamines, including methamphetamine, in contrast with 15 million users of cocaine and ~10 million users of heroin (United Nations Office on Drug and Crime, 2003). MA is an addictive CNS stimulant, and repeated use of MA causes long-term damage to dopaminergic and serotonergic fiber pathways in the brain (Ricaurte et al., 1980; Commins and Seiden, 1986). MA releases dopamine from vesicular storage pools into the cytoplasm, where it can be oxidized to produce neurotoxic quinones and additional reactive oxygen species that are thought to cause neurite degeneration (Larsen et al., 2002). Pubill et al. (2003) found that MA (four

injections of 10 mg/kg, s.c., at 2 hr intervals) induced 35% loss of dopaminergic terminals, generally without cell death, and astrogliosis in the striatum, cortex, and hippocampus of the rat. In MA-treated rats, Kokoshka et al. (1998) also found a loss of dopamine transporters in striatal synaptosomes.

A body of literature on how MA interacts with the structure and chemistry of the human brain is also emerging. Studies using structural magnetic resonance imaging (MRI) (Yen et al., 1994; Perez et al., 1999), single photon emission computed tomography (Kao et al., 1994; Iyo et al., 1997), and proton magnetic resonance spectroscopy (Ernst et al., 2000) have suggested that MA produces detrimental effects. Positron emission tomography (PET) has demonstrated that compared with corresponding measures in control subjects, MA abusers exhibit lower levels of dopamine transporters in the striatum (McCann et al., 1998; Sekine et al., 2001; Volkow et al., 2001) and prefrontal cortex (Sekine et al., 2003) and differences in regional cerebral glucose metabolism (Volkow et al., 2001; London et al., 2004). In a subsample of the participants in the present study, who underwent PET scanning to assay cerebral glucose metabolism, MA abusers in early abstinence had impairments in anterior cingulate, insular, and amygdalar regions of cortex that correlated with self reports of negative affective states (London et al., 2004). Other brain-imaging studies of MA abusers have found alterations in

Table 1. Characteristics of research participants

	Controls ($n = 21$)	MA abusers ($n = 22$)
Age (years)[a]	31.9 (1.47)	35.3 (1.66)
Gender (males/females)	10/11	15/7
Education (years)[a]	15.2 (0.50)	12.8 (0.42)*
Mother's education (years)[a,b]*	14.2 (0.48)	13.0 (0.68)
Race		
Caucasian (non-Hispanic)	14	13
Caucasian (Hispanic)	3	5
African American	3	2
Asian	1	2
Handedness (right handed)[c]	16	17

[a]Data shown are means (SEM); $n = 21$ for controls; $n = 22$ for MA abusers.

[b]$n = 20$ for controls.

[c]Handedness was determined according to the Lateral Preference Pattern Assignment subtest of the Physical and Neurological Examination for Soft Signs (Denckla, 1985). To qualify as right handed, a participant had to write and to perform all or all but 1 of 11 items other than writing with the right hand.

*Significantly different from controls; $p < 0.001$ by Student's t test.

Table 2. Self-reported drug use[a]

	Controls ($n = 21$)	MA abusers ($n = 22$)
Methamphetamine use		
Duration (year)		10.5 (1.09); $n = 21$
Average (gm/week)		3.44 (0.79); $n = 19$
Days used in last 30 d		18.9 (1.75); $n = 21$
Age of first use (year)		26.1 (1.77); $n = 12$
Tobacco smokers		
(>5 cigarettes/d)	$n = 2$	$n = 15$*
Marijuana use		
Days used in last 30 d	0.14 (0.08); $n = 21$	2.38 (0.91);** $n = 21$
Alcohol use		
Days used in last 30 d	2.38 (0.69); $n = 21$	3.24 (0.85); $n = 21$

[a]Data shown are means (SEM) of self-reported drug use from an intake questionnaire, a drug-use survey, and the Addiction Severity Index (McLellan et al., 1992).

*Significantly different from controls by Pearson χ^2 analysis.

**Significantly different from control group; $p < 0.05$ by Student's t test.

perfusion (Chang et al., 2002), levels of neuronal metabolites (Ernst et al., 2000), and cortical activation (Paulus et al., 2002).

Few structural imaging studies have been conducted in MA abusers. Yet with MRI, detailed spatial maps of cortical morphology can be created, and gray- and white-matter integrity and subcortical atrophy can be assessed. We therefore undertook a detailed structural brain-imaging study of the cortical surface and key subcortical structures in MA abusers. Cortical surface anatomy was carefully matched across individuals to localize group differences in gray-matter relative to gyral landmarks over the entire cerebral surface. Based on previous findings of limbic metabolic deficits in a subsample of the subjects studied here (London et al., 2004), we predicted that we might find gray-matter deficits in limbic–paralimbic cortices, particularly the cingulate gyrus. Because neuropsychological assessments have also suggested that MA abusers may have memory impairments (Simon et al., 2000), we hypothesized that we might find deficits in deep temporal lobe structures that support learning and recall, including the hippocampus. Overall, our objective was to visualize the anatomical pattern of MA-induced deficits to determine whether these impairments are anatomically restricted and correlated with cognitive impairment.

Materials and Methods

Participants. Forty-three subjects were carefully screened for the study (Table 1). Twenty-two MA users with a history of MA dependence (mean age, 35.3 ± 1.7 years; 15 men and 7 women) and 21 comparison subjects without a history of substance abuse (mean age, 31.9 ± 1.5 years; 10 men and 11 women) were selected. Selection criteria were as described by London et al. (2004) and are detailed briefly here. Subjects in both groups were healthy according to physical examination, medical history, and laboratory tests (hematocrit, electrolytes, and markers of hepatic and renal function). Exclusion criteria included the following: use of psychoactive medications; cardiovascular, pulmonary, or systemic disease; and seropositive status for human immunodeficiency virus (HIV) infection. As established by the structured clinical interview for the *Diagnostic and Statistical Manual of Mental Disorders-IV* SCID-I (First et al., 1996), current Axis I diagnoses other than MA or nicotine dependence were exclusionary for the MA abuser group. The same criteria applied for control subjects, but MA dependence was not allowed and restrictions on drug abuse extended to lifetime diagnoses. Axis II disorders were not exclusionary. The groups did not differ significantly in age, but the MA abusers had slightly fewer years of education than the control subjects (15.2 years for controls vs 12.8 years for MA abusers). Informed consent was obtained from all participants, and the study was approved by the University of California Los Angeles Institutional Review Board.

Drug use. Participants completed self-report drug-use questionnaires

[intake questionnaire, drug-use survey, and Addiction Severity Index (McLellan et al., 1992)] (Table 2). The MA abusers had used the drug (primarily by smoking) for 10.5 years on average, beginning in their mid-twenties. They consumed ~3 gm of MA per week, having used MA on most of the 30 d before entering the study. The groups reported similar alcohol use (Table 2). Most of the MA abusers but only two of the controls, however, smoked tobacco cigarettes. All analyses were run with and without six MA subjects who reported remarkable levels of marijuana use (more than one joint per week or a history of marijuana dependence, as determined by the SCID-I interview). Although p values changed slightly, this did not affect whether each result was statistically significant, so we present results for the full sample.

Neuropsychological testing. To determine possible links between hippocampal atrophy and memory performance, episodic memory was evaluated using the repeated memory test (Simon, 1999). Briefly, this tests recall and recognition of pictures and words using stimuli from the Snodgrass and Vanderwart corpus (Snodgrass and Vanderwart, 1980). Twenty-five words and 25 line drawings were presented for 1 sec each. For the next 10 min, participants performed unrelated tasks designed to distract them [i.e., the digit symbol subtest of the Wechsler Adult Intelligence Scale, revised (Wechsler, 1981) and Trail-Making A and B (Reitan, 1958)]. Next, they were tested for recall and then for recognition. The recognition test consisted of the target words and pictures as well as an equal number of equivalent items from the Snodgrass and Vanderwart corpus (words equal in length and mean frequency in the language; pictures equal in rated complexity and familiarity, and also mean frequency in the language) to the target stimuli. Measures of the number correct for word recall, picture recall, word recognition, and picture recognition were retained for correlation with MRI measures of hippocampal atrophy.

Clinical assessment of mood and anxiety. Mood and anxiety measures were assessed as in our previous PET study (London et al., 2004). Self ratings were obtained for depressive symptoms (Beck Depression Inventory) (Beck and Steer, 1987) and anxiety (State-Trait Anxiety Inventory) (Spielberger, 1983) and are reported in Table 3.

MRI scans. All subjects were scanned (by E.D.L.) with a single 3.0 tesla superconducting magnet (GE Medical Systems, Waukesha, WI), located at University of California Los Angeles. Structural MRI scans were three-dimensional (3D) T1-weighted spoiled gradient-recalled acquisition volumes (256 × 256 matrix; echo time, 4 msec; repetition time, 24 msec; flip angle, 35°; slice thickness, 1.22 mm). All magnetic resonance images were processed with a series of manual and automated procedures that are described in detail in other reports and summarized below. [Cortical surface analyses are identical to those in Thompson et al. (2003), and hippocampal analyses are identical to those in Narr et al. (2002).]

Image processing. First, each image volume was resliced into a standard orientation by a trained operator (K.M.H.) who "tagged" 20 standardized anatomical landmarks in each subject's image data set that corresponded to the same 20 anatomical landmarks defined on the International Consortium for Brain Mapping-305 average brain (Thompson et

Table 3. Self reports of mood and feeling state[a]

	Control subjects (n = 21)	MA abusers (n = 22)
Beck Depression Inventory		
Sample size	20	22
Mean score	1.25 (1.25)	9.77 (1.89)[b]*
Mean days abstinent (SD)		6.64 (5.2)
Spielberger State-Trait Anxiety Inventory		
Sample size	15	15
State anxiety score	31.4 (3.77)	38.67 (2.64)**
Trait anxiety score	31.9 (2.41)	38.7 (2.63)***

[a]Data are expressed as means (SEM). Beck Depression Inventory scores range from 0 to 63. Spielberger State-Trait Anxiety Inventory scores are reported as the sum of 20 questions ranking anxiety on a scale of 1–4.

[b]Beck Depression Inventory scores were closely correlated with the days of abstinence at time of assessment; $p < 0.05$ by regression.

*Significantly different from controls; $p < 0.0005$ by Student's t test.

**Not significantly different from controls; $p = 0.0506$.

***Significantly different from controls; $p < 0.001$ by Student's t test.

al., 2003). Next, brain image volumes were spatially registered to each other more carefully by defining 80 standardized, manually defined anatomical landmarks (40 in each hemisphere, the first and last points on each of 20 sulcal lines drawn in each hemisphere described below) in every individual (Sowell et al., 2003). A least-squares, rigid-body transformation spatially matched each individual to the average of all of the healthy controls. In this way, every individual's brain was matched in space, but global differences in brain size and shape remained intact. Automated tissue segmentation was conducted for each volume data set to classify voxels as most representative of gray matter, white matter, CSF, or a background class (representing extracerebral voxels in the image), on the basis of signal intensity. The procedure fits a mixture of Gaussian distributions to the intensities in each image before assigning each voxel to the class with the highest probability. Nonbrain tissue (i.e., scalp, orbits) was removed from the spatially transformed, tissue-segmented images. Then each individual's cortical surface was extracted and three-dimensionally rendered using automated software (Mac-Donald et al., 2000). This software creates a mesh-like surface that is continuously deformed to fit a threshold intensity value for the cortical surface that was defined as the MRI signal value that best differentiated cortical CSF from the underlying cortical gray matter. Each resulting cortical surface was represented as a high-resolution mesh of 131,072 surface triangles spanning 65,536 surface points.

Anatomical analysis. An image-analysis technique known as cortical pattern matching (Thompson et al., 2003) was used to localize disease effects on cortical anatomy and increase the power to detect group differences. The approach models, and controls for, gyral pattern variations across subjects. A set of 72 sulcal landmarks per brain constrains the mapping of one cortex onto another. This associates corresponding cortical regions across subjects. An image analyst (K.M.H.), blind to subject diagnosis, gender, and age, traced each of 30 sulci in each hemisphere on the surface rendering of each subject's brain (13 on the medial surface, 17 on the lateral surface). On the lateral brain surface, these included the Sylvian fissure; central, precentral, and postcentral sulci; superior temporal sulcus (STS) main body; STS ascending branch; STS posterior branch; primary and secondary intermediate sulci; and inferior temporal, superior and inferior frontal, intraparietal, transverse occipital, olfactory, occipitotemporal, and collateral sulci. On the medial surface, these included the callosal sulcus, inferior callosal outline, paracentral sulcus, anterior and posterior cingulate sulci, outer segment of a double parallel cingulate sulcus (where present) (Ono et al., 1990), superior and inferior rostral sulci, parietooccipital sulcus, anterior and posterior calcarine sulci, and subparietal sulcus. In addition to contouring the major sulci, a set of six midline landmark curves bordering the longitudinal fissure was outlined in each hemisphere to establish hemispheric gyral limits. Spatially registered gray-scale image volumes in coronal, axial, and sagittal planes were available simultaneously to help disambiguate brain anatomy. Landmarks were defined according to a detailed anatomical protocol (Sowell et al., 2001) based on the sulcal atlas of Ono et al. (1990). These criteria, along with interrater reliability measures, have been described previously (Sowell et al., 2001), and the written anatomical protocol can be obtained at http://www.loni.ucla.edu/~khayashi/Public/medial_surface/.

Cortical gray-matter maps. Points on the cortical surfaces around and between the sulcal contours drawn on each individual's brain surface were calculated using the averaged sulcal contours as anchors to drive into correspondence the 3D cortical-surface mesh models from each subject (Thompson et al., 2003). This procedure creates average 3D surface models for the MA and control groups and creates group-average maps of various features of the brain surface, such as gray-matter density. In this averaging process, a cortical model with the average shape for the group is generated, and features from corresponding gyri are averaged together. To quantify local gray matter, we used a measure referred to as gray-matter density, used in many previous studies to compare the spatial distribution of gray matter across subjects (Wright et al., 1995; Ashburner and Friston, 2000; Thompson et al., 2003). This measures the proportion of gray matter in a small region of fixed radius (15 mm) around each cortical point. Given the large anatomic variability in some cortical regions, high-dimensional elastic matching of cortical patterns (Thompson and Toga, 2002) was used to associate measures of gray-matter density from homologous cortical regions across subjects. One advantage of cortical matching is that it localizes deficits relative to gyral landmarks. It also averages data from corresponding gyri, which would be impossible if data were only linearly mapped into stereotaxic space.

Briefly, a sphere with a radius of 15 mm, centered at each cortical surface point, was made and referenced to the same spatial location in the gray-matter maps for each subject, derived previously in the tissue classification. The proportion of segmented gray-matter voxels relative to the total number of voxels in this sphere was computed at each point and stored as a map of proportional gray matter (with possible values ranging from 0.0 to 1.0) for each subject. The proportion of gray matter in each sphere at each point in each individual is reflective, in part, of local cortical thickness that varies over different regions of the brain. Because the deformation maps (acquired during matching of the cortical surfaces) associate the corresponding anatomical features of the cortex across subjects (on the basis of sulcal contours drawn in each individual), a local measurement of gray-matter density at each point over the surface of the brain was calculated for each subject and averaged across corresponding regions of cortex.

Mapping gray-matter loss. Statistical maps were generated, indicating group differences in local gray-matter volumes. To do this, a multiple regression was run at each cortical point to assess whether the quantity of gray matter at that point depended on group membership. The p value describing the significance of this linkage was plotted at each point on the cortex using a color code to produce a statistical map (see Fig. 1). The statistical maps (uncorrected) are crucial for allowing us to visualize the spatial patterns of gray-matter deficits, but permutation methods (Bullmore et al., 1999; Thompson et al., 2003) were used to assess the significance of the statistical maps and to correct for multiple comparisons. In each case, the covariate (group membership) was permuted 1,000,000 times on an SGI (Mountain View, CA) Reality Monster supercomputer with 32 internal R10000 processors, and a null distribution was developed for the area of the average cortex with group-difference statistics above a fixed threshold in the significance maps. An algorithm was then developed to report the significance probability for the overall loss patterns in each map as a whole (Thompson et al., 2003), after the appropriate correction for multiple comparisons.

Hippocampal maps. To assess hippocampal atrophy, we also created 3D surface models of the hippocampus in each scan, using criteria reported previously (Narr et al., 2002). The volumes of these 3D models were measured. To measure localized atrophy, a medial 3D curve was also derived from each individual hippocampus, threading down its central axis. The distance of each surface point from this centerline measures the radial size of the hippocampus. Regressions were run at each surface point to map linkages between radial size and memory scores. The resulting maps were visualized, and their significance was assessed by permutation to correct for multiple comparisons within each statistical map (Thompson et al., 2003).
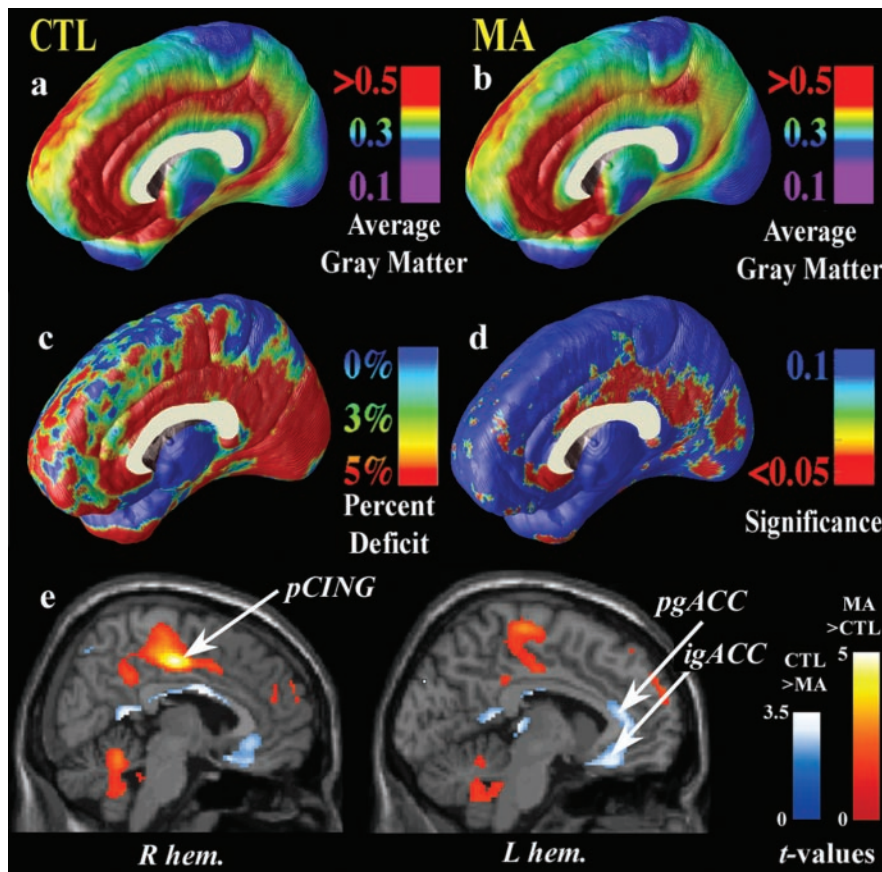
Figure 1. Gray-matter differences on the medial brain surface. Group difference maps (*c*) show mean percentage differences in gray-matter volumes between the control group average (*a*) and the methamphetamine group average (*b*), according to the color bar. The significance of these reductions is plotted in *d* as a map of *p* values. The cingulate gyrus shows highly significant gray-matter deficits (red colors; $p < 0.034$, corrected), whereas other brain regions are comparatively spared (blue colors). *e* is from London et al. (2004) (reprinted with permission). It shows the locations of MA ($n = 17$) and control ($n = 18$) group differences in relative regional cerebral metabolic glucose rate, assessed with PET. This PET sample partially overlaps with the current sample assessed with MRI. Briefly, in *e*, statistical parametric maps reveal regions in which the MA group has greater (red colors) or lesser (blue colors) glucose metabolism. Colors superimposed on a gray-scale MRI template indicate areas in which the significance of the group difference was $t \geq 1.69$ ($p = 0.049$). The region of greatest gray-matter deficit (*b*, *d*) is in the right hemisphere posterior cingulate cortex (pCING), and so is the region of greatest metabolic increase in the MA group (*e*). This suggests an anatomical congruence of the MRI-based deficits with metabolic differences observed with PET. igACC and pgACC denote the inferior and perigenual anterior cingulate cortex, respectively. CTL, Control; R hem, right hemisphere; L hem, left hemisphere.
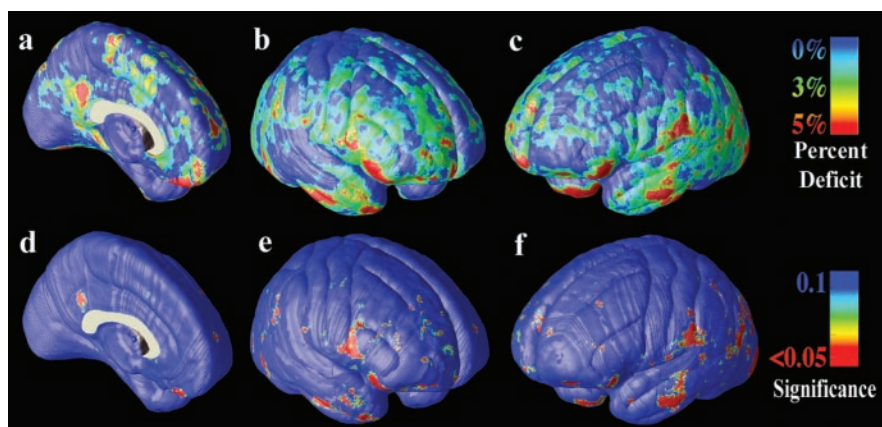

Figure 2. Gray-matter differences on the lateral brain surfaces. The mean reduction in gray matter in the MA group, relative to healthy controls, is expressed as a percentage and shown color-coded (blue colors, no reduction; red colors, greater reduction). In the left medial wall (*a*) and right-lateral (*b*) and left-lateral (*c*) brain surfaces, gray-matter differences are not pronounced. The significance of these differences is plotted in *d*–*f*. Differences were not significant after correction for multiple comparisons.
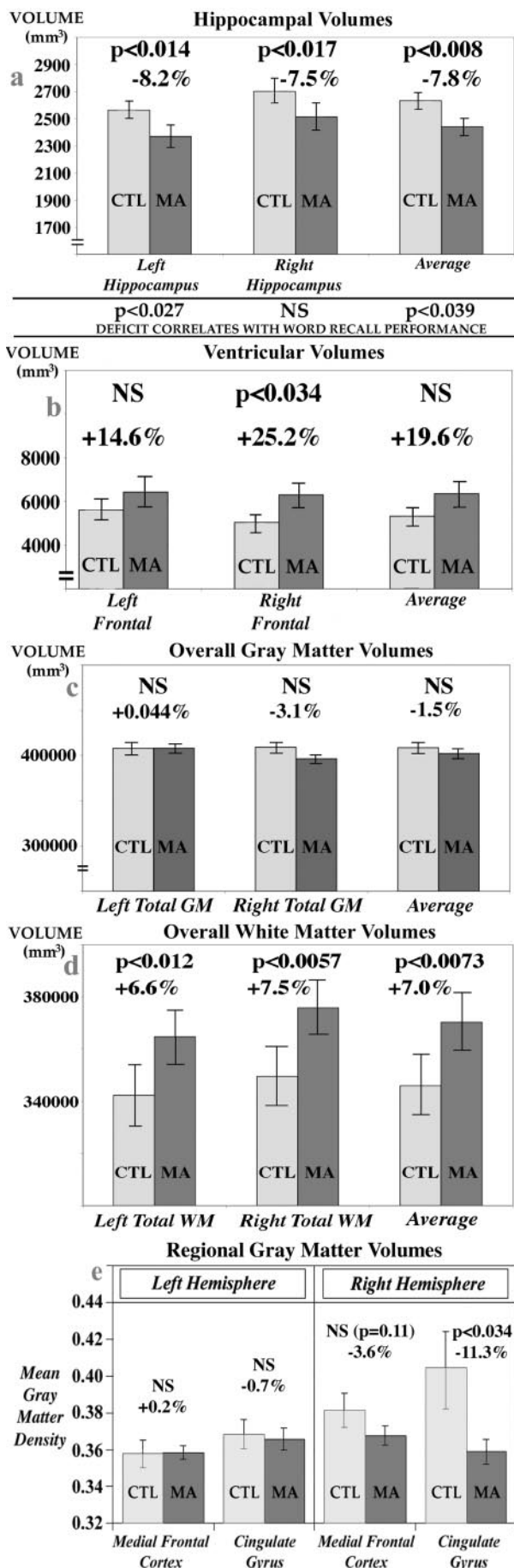
Results

Mapping cortical gray-matter deficits

In MA abusers, a highly significant gray-matter deficit was observed in a broad anatomical region encompassing the cingulate gyrus, subgenual cortex, and paralimbic belts, which form a ring of cortex encircling the corpus callosum ($p < 0.05$, corrected, for an effect of MA use; permutation test) (Fig. 1*a*–*d*). The most significant impairments occurred in cingulate regions (Fig. 1*d*, red colors), in which gray-matter volumes were 11.3% below the control average ($p < 0.05$). Most intriguing was the anatomical specificity of the loss. A sharp division occurred in the loss maps (Fig. 1*d*, blue colors), with medial frontal cortices displaying only a trend for loss (3.6% average reduction; $p < 0.1$) compared with the limbic cortices that they surround (Fig. 1*c*). Although the right medial wall displayed severe deficits, corresponding regions of the left hemisphere and lateral surfaces of both brain hemispheres did not exhibit gray-matter reductions (the 0.7% mean gray-matter reduction in the left cingulate of MA abusers was not significant; $p = 0.4$) (Fig. 2). Intriguingly, the MRI-based maps of gray-matter deficits were highly congruent with previously reported maps of group differences in glucose metabolism in a partially overlapping sample [Fig. 1*e*, from London et al. (2004), reprinted with permission].

Hippocampal deficits

Hippocampal volumes were significantly smaller in MA abusers than in control subjects (average volume was 7.8% less; $p < 0.01$) (Fig. 3*a*). In multiple regressions that adjusted for potential effects of age and gender, *post hoc* tests revealed that both left and right hippocampi were severely atrophied (left hippocampus, −8.2% smaller, $p = 0.01$; right hippocampus, −7.5% smaller, $p < 0.05$). Although there were no group differences in total cerebral volume, the hippocampal deficits were maintained after adjusting for variance caused by individual differences in overall brain size. In that case, total ($p < 0.01$), left ($p < 0.05$), and right ($p < 0.05$) hippocampal volumes were still all significantly smaller in the MA group. To be sure that the effect was not attributable to the six MA users who also used marijuana frequently (as noted above), we ran separate analyses that excluded them from the MA group and found exactly the same deficits (all $p < 0.05$ for total, left, and right hippocampal volumes). These volume deficits were associated with poorer memory perfor-

mance as well. Both total ($p < 0.05$) and right ($p < 0.05$) hippocampal volumes were positively correlated with performance on a word-recall task (Fig. 3a); subjects who had smaller volumes performed more poorly. Radial atrophy of the left hippocampus (Fig. 4) was significantly associated with group membership (greater atrophy in the MA group; $p < 0.05$) and word-recall performance (greater atrophy correlated with poorer performance; $p = 0.01$; $p < 0.05$, corrected for multiple comparisons). Tests of picture recall as well as word and picture recognition were also conducted, but these cognitive measures were not found to correlate with MRI measures of hippocampal atrophy.

Whole-brain gray- and white-matter measures

We also wanted to determine whether the group differences in gray-matter volume in the hippocampus and paralimbic belt simply reflected a generalized gray-matter atrophy or were restricted to those structures. There were no group differences in total cerebral volumes or total gray matter ($p > 0.1$) (Fig. 2c). Surprisingly, we found significant hypertrophy of the white matter in the MA group (Fig. 2d). Total white-matter volumes were 7.0% greater in MA abusers than controls ($p < 0.01$), with a 6.6% white-matter excess in the left hemisphere ($p = 0.01$) and a 7.5% excess in the right hemisphere ($p < 0.01$). After partitioning the white matter into lobes, we also conducted *post hoc* tests to determine where white-matter hypertrophy was prominent. MA abusers had hypertrophy of the temporal white matter (left, $p < 0.005$; right, $p < 0.05$) and occipital white matter (left, $p < 0.05$; right, $p < 0.01$), adjacent to some of the same regions in which hippocampal and cortical gray-matter changes were detected. Finally, we noted that the right cingulate gray-matter loss accompanied significant frontal horn expansion in the right lateral ventricles (25.2% expansion; $p < 0.05$) (Fig. 2b). This expansion effect typically accompanies gray-matter atrophy and is part of a structural pattern often found in neurodegenerative or psychotic disorders (Thompson et al., 2003).

Lateralization of cingulate deficits

To examine the apparent lateralization of gray-matter deficit to the right medial cortical surface, we wanted to determine whether (1) the methamphetamine group had a greater percentage deficit in the right cingulate, or (2) a comparable deficit in the left cingulate had simply been obscured by greater anatomical variance on that side. The first case appears to be true. Figure 3e shows the average gray-matter density in the left and right cingulate gyrus in patients and controls. If only the cingulate gyrus is considered, in patients the mean gray-matter density is 11.3% lower on the right ($p < 0.05$) but not significantly lower on the left (0.7%; $p > 0.1$). Furthermore, there is a significant right $>$ left asymmetry in normal cingulate gray-matter density ($p < 0.05$; paired t test), as observed previously in the anterior cingulate in healthy controls ($n = 465$ subjects) (Good et al., 2001; Watkins et al., 2001). As

←

Figure 3. Comparison of brain structure volumes in MA abusers and healthy controls (CTL). Means and SE measures (error bars) are shown for the volumes of the hippocampus (a), frontal horn of the lateral ventricles (b), total cerebral gray matter (GM) (c), and total cerebral white matter (WM) (d). MA abusers show reductions in hippocampal volumes without significant reductions in gray-matter volume overall (c). They also show volume expansions in some ventricular regions (b) and increases in white-matter volume (d). e shows that mean gray-matter density in the cingulate gyrus is reduced in MA abusers (by 11.3%; $p < 0.034$), erasing the normal right $>$ left asymmetry in gray-matter density that is found here and has been documented previously in healthy subjects. In agreement with the maps, this deficit pattern is not found in the adjacent medial frontal cortex.
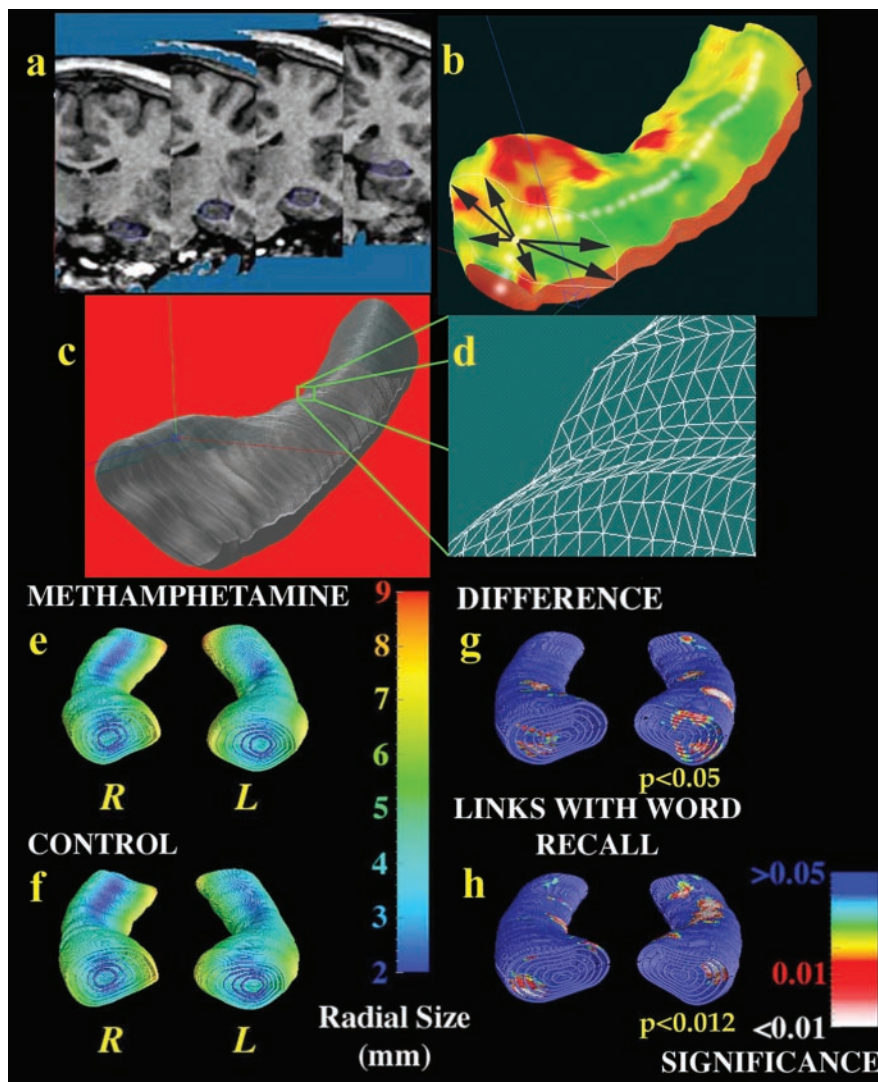
Figure 4. Hippocampal atrophy in MA abusers is linked with poorer memory performance. Each individual's hippocampus is traced in coronal MRI sections (*a*) and converted to a mesh surface representation (*b*) in which the radial size of the hippocampus is measured from a centerline and plotted in color on the surface to index radial atrophy. Arrows in *b* represent vectors from the centerline to various points on the hippocampal surface. These meshes are averaged across subjects (*c*), and atrophy relative to the control mean is computed at each surface grid point (*d*). Shown in millimeters in *e* and *f*, the average radial size of the hippocampus in MA abusers (*e*) is smaller in some regions [red colors in *g*] than corresponding regions in healthy controls (*f*). *h* shows hippocampal regions (in red colors) in which word-recall performance is significantly linked with radial atrophy.

shown in Figure 3*e*, the deficit in the methamphetamine group appears to erase the right > left asymmetry found in controls, affecting the right side more severely. In agreement with the maps, the reduction in gray-matter density is greater in the cingulate cortex (11.3%) than in the adjacent medial frontal cortex (3.6%) (Fig. 3*e*), where no normal gray-matter asymmetry was detected.

Discussion

These maps reveal three key alterations in brain structure in MA abusers. First, a broad cingulate and limbic deficit in gray-matter concentration appears prominently in the right hemisphere and is accompanied by expansion of the underlying ventricles. Second, MA abusers had a 7.8% deficit in hippocampal volume, and individual volumes were correlated with memory performance on a word-recall task, in that subjects with smaller hippocampi performed more poorly. Third, we found a prominent white-

matter hypertrophy (i.e., a 7.0% increase in white-matter volume) that was also highly significant in the temporal regions that surround the hippocampus. These changes are remarkable, because they show that chronic MA abuse is associated with a pattern of abnormal brain structure that is comparable with or greater than MRI deficits in early dementia and schizophrenia in terms of effect size. Nonetheless, the components of the structural change are likely different, and it is possible that larger changes may actually be more benign. Lawrie and Abukmeil (1998) found an average 5.5% hippocampal volume deficit in a meta-analysis of MRI studies of schizophrenic adults. Alzheimer's disease patients typically show a similar, selective loss of hippocampal and limbic gray matter that correlates tightly with cognitive decline on the Mini-Mental State Exam (Thompson et al., 2003). Active MA users often exhibit performance deficits on tests of verbal memory, as well as tests of perceptual motor speed and executive functions such as inhibition, problem solving, abstract thinking, and tasks that require mental flexibility (Simon et al., 2002). Abstinent users show impaired response inhibition (Salo et al., 2002; Kalechstein et al., 2003) and decision-making (Paulus et al., 2002). Even so, the memory deficit is not found in all studies; some studies find deficits (Simon et al., 2002; Kalechstein et al., 2003), whereas others find performance in the normal range (Chang et al., 2002). Tests of picture recall and well as word and picture recognition were also conducted, and these cognitive measures were not significantly linked with MRI measures of atrophy. Nonetheless, the link between hippocampal atrophy and word recall remained significant even after Bonferroni correction for the number of tests conducted (four tests; $p = 0.01$, uncorrected; $p < 0.05$, corrected). Links between hippocampal atrophy and episodic memory may be somewhat specific to word recall, but correlations with other neuropsychological measures may be detectable in a larger cohort than that examined here.

MA induces an unusual type of neurodegeneration in which axonal arbors of dopamine neurons are destroyed but cell bodies are not lost (Ricaurte et al., 1980). The midbrain dopamine system has strong projections from the substantia nigra and ventral tegmentum to the cingulate and limbic association cortex, which appears here to degenerate preferentially. MA also may be especially neurotoxic to limbic structures that underlie memory and recall, because there are strong serotonergic projections from the raphe nuclei to the hippocampus (Donovan et al., 2002), which is severely atrophied here.

The selective atrophy of the right cingulate gyrus in the methamphetamine group appears to erase the right > left gray-matter asymmetry found here in controls (Fig. 3*e*). This normal asym-

metry in the cingulate cortex has also been documented for the anterior cingulate in large samples of healthy subjects scanned with MRI (Good et al., 2001; Watkins et al., 2001). Intriguingly, this normal gray-matter asymmetry is also erased in schizophrenia patients, who may also exhibit cingulate gray-matter deficits (Takahashi et al., 2002). Normal anatomic asymmetries in the cingulate suggest that there may be specific classes of cortical neurons that are asymmetrically represented between the brain hemispheres. This could result in an apparent differential vulnerability of the cortex at a gross anatomic level even if the chronic effects on specific cell types were uniform. Additional studies at a cellular level are required to reveal whether methamphetamine affects these limbic cell populations uniformly or whether there is a genuinely lateralized atrophic process, as may occur in neurodegenerative conditions such as Alzheimer's disease (Thompson et al., 2003).

The relationship between impaired structure and metabolism is also of interest. In a PET study of subjects who overlapped with the current groups (London et al., 2004), the cingulate cortex had the most robust deficits in relative glucose metabolism, and this region stands out as having the greatest structural atrophy here as well. As shown in Figure 1b,d,e, the most significant gray-matter atrophy occurred in the right posterior cingulate, the same anatomical region with the greatest increase in glucose metabolism in the MA group (London et al., 2004). Because the cingulate gyrus contributes to both emotional and cognitive functions (for review, see Vogt et al., 2003), the structural abnormality found throughout this gyrus may underlie a variety of behavioral problems of MA abusers. In PET studies, activation of the anterior cingulate gyrus is associated with drug craving (Maas et al., 1998, Childress et al., 1999; Garavan et al., 2000; Kilts et al., 2001; Wexler et al., 2001; Bonson et al., 2002; Brody et al., 2002), and the anterior cingulate is implicated in primary depression and induction of sadness (Drevets, 2000; Vogt et al., 2003). The importance of anterior cingulate dysfunction in MA abuse has been documented by the correlation of self reports of depressive symptoms with relative glucose metabolism (London et al., 2004). Compared with control subjects, MA abusers gave higher self ratings of their depressive symptoms, which covaried positively with relative metabolism in the perigenual anterior cingulate gyrus, and of anxiety (state and trait measures), which covaried negatively with relative activity of the anterior cingulate cortex. Furthermore, in light of the role of the cingulate gyrus in inhibitory control and deficits in performance of tasks that require such control in MA abusers (Goldstein and Volkow, 2002), the structural abnormalities reported here, paired with the metabolic abnormalities (in the perigenual, infragenual, and posterior areas of the cingulate gyrus) (London et al., 2004), suggest a substrate for cognitive disorder that could interfere with treatment of MA dependence. MA abusers abstinent for 2–4 months also exhibit greater interference than control subjects on the Stroop task (Salo et al., 2002), which has involved activation of the anterior cingulate gyrus (Cabeza and Nyberg, 2000).

White-matter hypertrophy, found here unexpectedly, may reflect adaptive glial changes or altered myelination in response to repeated drug exposure. In a recent abstract, Jernigan et al. (2003) also found enlarged lobar volumes in an independent sample of MA abusers, recruited as part of an ongoing HIV study. One important question is whether these apparent gains in white-matter volumes might be attributable to MRI signal or volume changes in the adjacent cortical gray matter (Bookstein, 2001). Gray-matter loss alone would not explain the greater part of the white-matter volume gains, because the net gain in white-matter

volume (mean, 24.3 cc) is much greater than the overall gray-matter reduction (mean, 6.3 cc). This suggests that there is some additional process (perhaps adaptive glial changes or altered myelination) that must explain the white-matter hypertrophy. Although the magnitude of the changes was unexpected [with a 6.6% white-matter excess in the left hemisphere ($p = 0.01$) and a 7.5% excess in the right hemisphere ($p < 0.001$)], gliosis is known to occur with methamphetamine abuse, as with all forms of neuronal damage (Escubedo et al., 1998). These glial changes may contribute to the white-matter volume increases observed here.

Our study participants were in their thirties, ~15 years younger than the age when white-matter volume is usually greatest (Bartzokis et al., 2001, 2003). MA-induced gray-matter losses with white-matter gains somewhat resemble an exaggerated pattern of normal aging, but the white-matter changes are large enough to suggest that they may be compensatory or pathological reactions to chronic drug exposure. In addition to perfusion deficits in the striatum, the MA study by Chang et al. (2002) reported compensatory excess perfusion (relative to controls) in left temporoparietal white matter, occipital brain regions, and right posterior parietal lobes. Reactive increases in regional cerebral blood flow may be attributable to increased glial activity as well as astrogliosis (proliferation in response to brain injury).

Significance maps

When maps of significance probabilities are presented, we followed the somewhat standard procedure in brain mapping in which a corrected p value is computed for the entire anatomical map. In other words, it is typical to show a fine-grained map of probabilities on the surface of the hippocampus (or more typically, an image with a separate probability value at each pixel) and then to give an overall corrected p value that indicates how likely it is that the observed pattern of group differences could have occurred by accident. For the maps of group differences in the hippocampus and cortex, we report a significance map and an overall significance value for the map (which is corrected for the multiple spatial comparisons). Of the two standard corrections for multiple spatial comparisons (parametric and nonparametric), we chose a nonparametric correction (permutation testing) to avoid making any assumptions about the error covariance structure, which is spatially correlated (Thompson et al., 2002).

The anatomical resolution of the statistical maps is of interest. Strictly speaking, it is possible to distinguish effects on the cortex that differentially affect adjacent gyri, because the cortical pattern-matching procedure pools data from homologous cortical regions across subjects, using a large set of sulcal landmarks as constraints. This gyrus-level resolution is diminished in regions in which sulcal landmarks poorly reflect functional or cellular subdivisions in the cortex. Nonetheless, a clear deficit pattern that is not apparent in the surrounding cortex is resolved in limbic areas. If additional functional landmarks in the cortex or hippocampus could be defined with imaging modalities other than MRI, they could be used to obtain still higher anatomical resolution by further constraining the correspondences invoked in creating group maps.

Cortical pattern matching

The cortical pattern-matching approach used here (Thompson et al., 2003) has some strengths and weaknesses relative to voxel-based morphometry (VBM) (Ashburner and Friston, 1999, 2000; Salmond et al., 2002). VBM also creates maps of gray-matter differences by aligning gray-matter images and comparing them

across groups, without creating surface models of anatomy. Although VBM is highly automated and can map effects on gray matter in large samples, it is less sensitive to detecting group effects on anatomy in highly variable anatomical regions. Our method, cortical pattern matching, provides a higher-order matching of cortical anatomy before making cross-subject comparisons. To match cortical landmarks with the highest possible accuracy across subjects, 3D geometric models of the cortex are extracted, and large networks of neuroanatomical landmarks are explicitly identified (i.e., sulcal curves in the cortex). Statistical effects on anatomy are then localized relative to gyral anatomy, controlling for anatomical variation across subjects and groups, and offering increased power to detect effects in highly variable anatomical regions.

To our knowledge, this study is the first to demonstrate systematic brain structural deficits in MA abusers. It has some limitations, however. It is not yet clear how these deficits emerge over time, whether they are progressive, and to what extent therapy or abstinence may reverse them. Another potential limitation relates to matching of the two groups. Although the groups were well matched on most categories, most of the MA abusers and only two of the control subjects were tobacco smokers. A recent study of brain structure found that smokers had smaller gray-matter volumes and lower gray-matter densities than nonsmokers in the prefrontal cortex (primarily in the bilateral dorsolateral prefrontal cortex but also in the left ventrolateral prefrontal cortex), along with smaller volumes in the left dorsal anterior cingulate gyrus and lower gray-matter densities in the right cerebellum (Brody et al., 2004). The effect related to smoking in the cingulate gyrus (dorsal, mid-cingulate area) was much more restricted than the current finding, which extended through the entire cingulate gyrus. Furthermore, no evidence of hippocampal abnormality was observed.

Future studies will relate these structural changes to known metabolic changes and depletions in dopamine and serotonin receptor or transporter densities. In these efforts, structural (and functional) MRI may offer valuable biomarkers to gauge cortical and hippocampal integrity. Future interventional studies are likely to clarify how these deficits relate to clinical prognosis.

References

Ashburner J, Friston KJ (1999) Nonlinear spatial normalization using basis functions. Hum Brain Mapp 7:254–266.

Ashburner J, Friston KJ (2000) Voxel-based morphometry–the methods [review]. NeuroImage 11:805–821.

Bartzokis G, Beckson M, Lu PH, Nuechterlein KH, Edwards N, Mintz J (2001) Age-related changes in frontal and temporal lobe volumes in men: a magnetic resonance imaging study. Arch Gen Psychiatry 58:461–465.

Bartzokis G, Cummings JL, Sultzer D, Henderson VW, Nuechterlein KH, Mintz J (2003) White matter structural integrity in healthy aging adults and patients with Alzheimer disease: a magnetic resonance imaging study. Arch Neurol 60:393–398.

Beck AT, Steer RA (1987) Manual for the Revised Beck Depression Inventory. San Antonio, TX: Psychological Corp.

Bonson KR, Grant SJ, Contoreggi CS, Links JM, Metcalfe J, Weyl HL, Kurian V, Ernst M, London ED (2002) Neural systems and cue-induced cocaine craving. Neuropsychopharmacology 26:376–386.

Bookstein FL (2001) "Voxel-based morphometry" should not be used with imperfectly registered images. NeuroImage 14:1454–1462.

Brody AL, Mandelkern M, London ED, Childress AR, Lee GS, Bota RG, Ho ML, Saxena S, Baxter LR, Madsen D, Jarvik ME (2002) Brain metabolic changes during cigarette craving. Arch Gen Psychiatry 59:1162–1172.

Brody AL, Mandelkern MA, Jarvik ME, Lee GS, Smith EC, Huang JC, Bota RG, Bartzokis G, London ED (2004) Differences between smokers and non-smokers in regional gray matter volumes and densities. Biol Psychiatry 55:77–84.

Bullmore ET, Suckling J, Overmeyer S, Rabe-Hesketh S, Taylor E, Brammer MJ (1999) Global, voxel, and cluster tests, by theory and permutation, for a difference between two groups of structural MR images of the brain. IEEE Trans Med Imaging 18:32–42.

Cabeza R, Nyberg L (2000) Imaging cognition II: an empirical review of 275 PET and fMRI studies [review]. J Cogn Neurosci 12:1–47.

Chang L, Ernst T, Speck O, Patel H, DeSilva M, Leonido-Yee M, Miller EN (2002) Perfusion MRI and computerized cognitive test abnormalities in abstinent methamphetamine users. Psychiatry Res 114:65–79.

Childress AR, Mozley PD, McElgin W, Fitzgerald J, Reivich M, O'Brien CP (1999) Limbic activation during cue-induced cocaine craving. Am J Psychiatry 156:11–18.

Commins DL, Seiden LS (1986) Alpha-methyltyrosine blocks methylamphetamine-induced degeneration in the rat somatosensory cortex. Brain Res 365:15–20.

Denckla MB (1985) Revised neurological examination for subtle signs. Psychopharmacol Bull 21:773–800.

Donovan SL, Mamounas LA, Andrews AM, Blue ME, McCasland JS (2002) GAP-43 is critical for normal development of the serotonergic innervation in forebrain. J Neurosci 22:3543–3552.

Drevets WC (2000) Functional anatomical abnormalities in limbic and prefrontal cortical structures in major depression [review]. Prog Brain Res 126:413–431.

Ernst T, Chang L, Leonido-Yee M, Speck O (2000) Evidence for long-term neurotoxicity associated with methamphetamine abuse: a 1H MRS study. Neurology 54:1344–1349.

Escubedo E, Guitart L, Sureda FX, Jimenez A, Pubill D, Pallas M, Camins A, Camarasa J (1998) Microgliosis and down-regulation of adenosine transporter induced by methamphetamine in rats. Brain Res 814:120–126.

First MB, Spitzer RL, Gibbon M, Williams J (1996) Structured Clinical Interview for DSM-IV Axis I disorders. Patient Edition (SCID-IP, version 2.0). New York: Biometrics Research Department, New York State Psychiatric Institute.

Garavan H, Pankiewicz J, Bloom A, Cho JK, Sperry L, Ross TJ, Salmeron BJ, Risinger R, Kelley D, Stein EA (2000) Cue-induced cocaine craving: neuroanatomical specificity for drug users and drug stimuli. Am J Psychiatry 157:1789–1798.

Goldstein RZ, Volkow ND (2002) Drug addiction and its underlying neurobiological basis: neuroimaging evidence for the involvement of the frontal cortex [review]. Am J Psychiatry 159:1642–1652.

Good CD, Johnsrude I, Ashburner J, Henson RN, Friston KJ, Frackowiak RS (2001) Cerebral asymmetry and the effects of sex and handedness on brain structure: a voxel-based morphometric analysis of 465 normal adult human brains. NeuroImage 14:685–700.

Iyo M, Namba H, Yanagisawa M, Hirai S, Yui N, Fukui S (1997) Abnormal cerebral perfusion in chronic methamphetamine abusers: a study using 99MTc-HMPAO and SPECT. Prog Neuropsychopharmacol Biol Psychiatry 21:789–796.

Jernigan TL, Archibald SL, Gamst AC, Fennema-Notestine C, Grant I, Ellis RO (2003) Effects of HIV, age, and methamphetamine abuse on brain structure. Soc Neurosci Abstr 29:135.1.

Kalechstein AD, Newton TF, Green M (2003) Methamphetamine dependence is associated with neurocognitive impairment in the initial phases of abstinence. J Neuropsychiatry Clin Neurosci 15:215–220.

Kao CH, Wang SJ, Yeh SH (1994) Presentation of regional cerebral blood flow in amphetamine abusers by 99Tcm-HMPAO brain SPECT. Nucl Med Commun 15:94–98.

Kilts CD, Schweitzer JB, Quinn CK, Gross RE, Faber TL, Muhammad F, Ely TD, Hoffman JM, Drexler KP (2001) Neural activity related to drug craving in cocaine addiction. Arch Gen Psychiatry 58:334–341.

Kokoshka JM, Vaughan RA, Hanson GR, Fleckenstein AE (1998) Nature of methamphetamine-induced rapid and reversible changes in dopamine transporters. Eur J Pharmacol 361:269–275.

Larsen KE, Fon EA, Hastings TG, Edwards RH, Sulzer D (2002) Methamphetamine-induced degeneration of dopaminergic neurons involves autophagy and upregulation of dopamine synthesis. J Neurosci 22:8951–8960.

Lawrie SM, Abukmeil SS (1998) Brain abnormality in schizophrenia. A systematic and quantitative review of volumetric magnetic resonance imaging studies [review]. Br J Psychiatry 172:110–120.

London ED, Simon SL, Berman SM, Mandelkern MA, Lichtman AM, Bramen J, Shinn AK, Miotto K, Learn J, Dong Y, Matochik JA, Kurian V, Newton

T, Woods RP, Rawson R, Ling W (2004) Regional cerebral dysfunction associated with mood disturbances in abstinent methamphetamine abusers. Arch Gen Psychiatry 61:73–84.

Maas LC, Lukas SE, Kaufman MJ, Weiss RD, Daniels SL, Rogers VW, Kukes TJ, Renshaw PF (1998) Functional magnetic resonance imaging of human brain activation during cue-induced cocaine craving. Am J Psychiatry 155:124–126.

MacDonald D, Kabani N, Avis D, Evans AC (2000) Automated 3-D extraction of inner and outer surfaces of cerebral cortex from MRI. NeuroImage 12:340–356.

McCann UD, Wong DF, Yokoi F, Villemagne V, Dannals RF, Ricaurte GA (1998) Reduced striatal dopamine transporter density in abstinent methamphetamine and methcathinone users: evidence from positron emission tomography studies with [^{11}C]WIN-35,428. J Neurosci 18:8417–8422.

McLellan AT, Kushner H, Metzger D, Peters R, Smith I, Grissom G, Pettinati H (1992) The Fifth Edition of the Addiction Severity Index. J Subst Abuse Treat 9:199–213.

Narr KL, van Erp TG, Cannon TD, Woods RP, Thompson PM, Jang S, Blanton R, Poutanen VP, Huttunen M, Lonnqvist J, Standerksjold-Nordenstam CG, Kaprio J, Mazziotta JC, Toga AW (2002) A twin study of genetic contributions to hippocampal morphology in schizophrenia. Neurobiol Dis 11:83–95.

Ono M, Kubik S, Abernathey CD (1990) Atlas of the cerebral sulci. Stuttgart, Germany: Thieme.

Paulus MP, Hozack NE, Zauscher BE, Frank L, Brown GG, Braff DL, Schuckit MA (2002) Behavioral and functional neuroimaging evidence for prefrontal dysfunction in methamphetamine-dependent subjects. Neuropsychopharmacology 26:53–63.

Perez JA, Arsura EL, Strategos S (1999) Methamphetamine-related stroke: four cases. J Emerg Med 17:469–471.

Pubill D, Canudas AM, Pallas M, Camins A, Camarasa J, Escubedo E (2003) Different glial response to methamphetamine- and methylenedioxy-methamphetamine-induced neurotoxicity. Naunyn Schmiedebergs Arch Pharmacol 367:490–499.

Reitan RM (1958) Validity of the trail making test as an indicator of organic brain damage. Percept Mot Skills 8:271–276.

Ricaurte GA, Schuster CR, Seiden LS (1980) Long-term effects of repeated methylamphetamine administration on dopamine and serotonin neurons in the rat brain: a regional study. Brain Res 193:153–163.

Salmond CH, Ashburner J, Vargha-Khadem F, Connelly A, Gadian DG, Friston KJ (2002) The precision of anatomical normalization in the medial temporal lobe using spatial basis functions. NeuroImage 17:507–512.

Salo R, Nordahl TE, Possin K, Leamon M, Gibson DR, Galloway GP, Flynn NM, Henik A, Pfefferbaum A, Sullivan EV (2002) Preliminary evidence of reduced cognitive inhibition in methamphetamine-dependent individuals. Psychiatry Res 111:65–74.

Sekine Y, Iyo M, Ouchi Y, Matsunaga T, Tsukada H, Yoshikawa E, Futatsubashi M, Takei N, Mori N (2001) Methamphetamine-related psychiatric symptoms and reduced brain dopamine transporters studied with PET. Am J Psychiatry 158:1206–1214.

Sekine Y, Minabe Y, Ouchi Y, Takei N, Iyo M, Nakamura K, Suzuki K, Tsukada H, Yoshikawa E, Futatsubashi M, Mori N (2003) Association of dopamine transporter loss in the orbitofrontal and dorsolateral prefrontal cortex with methamphetamine-related psychiatric symptoms. Am J Psychiatry 160:1699–1701.

Simon SL (1999) Repeated memory test. In: Treatment for stimulant use disorders, pp 207–218. Rockville, MD: United States Department of Health and Human Services.

Simon SL, Domier C, Carnell J, Brethen P, Rawson R, Ling W (2000) Cognitive impairment in individuals currently using methamphetamine. Am J Addict 9:222–231.

Simon SL, Domier CP, Sim T, Richardson K, Rawson RA, Ling W (2002) Cognitive performance of current methamphetamine and cocaine abusers. J Addict Dis 21:61–74.

Snodgrass JG, Vanderwart M (1980) A standardized set of 260 pictures: norms for name agreement, image agreement, familiarity, and visual complexity. J Exp Psychol [Hum Learn] 6:174–215.

Sowell ER, Thompson PM, Tessner KD, Toga AW (2001) Mapping continued brain growth and gray matter density reduction in dorsal frontal cortex: inverse relationships during postadolescent brain maturation. J Neurosci 21:8819–8829.

Sowell ER, Peterson BS, Thompson PM, Welcome SE, Henkenius AL, Toga AW (2003) Mapping cortical change across the human lifespan. Nat Neurosci 6:309–315.

Spielberger CD (1983) Manual for the State-Trait Anxiety Inventory (Form Y). Palo Alto, CA: Consulting Psychologists.

Takahashi T, Suzuki M, Kawasaki Y, Kurokawa K, Hagino H, Yamashita I, Zhou SY, Nohara S, Nakamura K, Seto H, Kurachi M (2002) Volumetric magnetic resonance imaging study of the anterior cingulate gyrus in schizotypal disorder. Eur Arch Psychiatry Clin Neurosci 252:268–277.

Thompson PM, Toga AW (2002) A framework for computational anatomy. Comput Vis Sci 5:1–12.

Thompson PM, Hayashi KM, de Zubicaray G, Janke AL, Rose SE, Semple J, Herman D, Hong MS, Dittmer S, Doddrell DM, Toga AW (2003) Dynamics of gray matter loss in Alzheimer's disease. J Neurosci 23:994–1005.

United Nations Office on Drugs and Crime (2003) Ecstasy and amphetamines, Global Survey 2003. New York: United Nations.

Vogt BA, Berger GR, Derbyshire SW (2003) Structural and functional dichotomy of human midcingulate cortex. Eur J Neurosci 18:3134–3144.

Volkow ND, Chang L, Wang GJ, Fowler JS, Leonido-Yee M, Franceschi D, Sedler MJ, Gatley SJ, Hitzemann R, Ding YS, Logan J, Wong C, Miller EN (2001) Association of dopamine transporter reduction with psychomotor impairment in methamphetamine abusers. Am J Psychiatry 158:377–382.

Watkins KE, Paus T, Lerch JP, Zijdenbos A, Collins DL, Neelin P, Taylor J, Worsley KJ, Evans AC (2001) Structural asymmetries in the human brain: a voxel-based statistical analysis of 142 MRI scans. Cereb Cortex 11:868–877.

Wechsler D (1981) Manual for the Wechsler Adult Intelligence Scale, revised. New York: The Psychological Corporation.

Wexler BE, Gottschalk GH, Fulbright RK, Prohovnik I, Lacadie CM, Rounsaville BJ, Gore JC (2001) Functional magnetic resonance imaging of cocaine craving. Am J Psychiatry 158:86–95.

Wright IC, McGuire PK, Poline JB, Travere JM, Murray RM, Frith CD, Frackowiak RS, Friston KJ (1995) A voxel-based method for the statistical analysis of gray and white matter density applied to schizophrenia. NeuroImage 2:244–252.

Yen DJ, Wang SJ, Chen CC, Liao KK, Fuh JL, Hu HH (1994) Stroke associated with methamphetamine inhalation. Eur Neurol 34:16–22.